

Supplementary Information

Ultrasml Sn Nanodots Embedded inside N-Doped Carbon Microcages as High-Performance Lithium and Sodium Ion Battery Anodes†

Hangjun Ying,^{a,b} Shunlong Zhang,^a Zhen Meng,^{a,b} Zixu Sun,^a and Weiqiang Han^{a,c,*}

^a*Ningbo Institute of Materials Technology & Engineering, Chinese Academy of Sciences, Ningbo, P. R. China, 315201*

^b*University of Chinese Academy of Sciences, 19 A Yuquan Rd, Shijingshan District, Beijing, P. R. China, 100049*

^c*School of Materials Science and Engineering, Zhejiang University, Hangzhou, P. R. China, 310027*

*E-mail: hanwq@zju.edu.cn

Experimental Section

Material synthesis: Sn/N-doped carbon microcages composites were prepared *via* a simple spray drying process, followed by pyrolysis reduction. In briefly, 3.16 g ethylenediaminetetraacetic acid (EDTA, $\geq 99.5\%$, Sinopharm) and 0.15 g F-127 (Pluronic[®] F-127, Aldrich) were added in 200 ml deionized water. After adding 5 ml ammonium hydroxide ($\text{NH}_3 \cdot \text{H}_2\text{O}$, 28%, Alfa), the EDTA dissolves rapidly. Then 5 g NaCl and 3.5 g tin(IV) chloride pentahydrate ($\text{SnCl}_4 \cdot 5\text{H}_2\text{O}$, 98%, Aldrich) were dispersed in the solution. After stirring for 3 h, the Sn/C precursor was collected by spray drying method with the inlet air temperature of 210 °C. Next, the composite was annealed at 700 °C for 2 h in argon atmosphere to carbonize EDTA and reduce Sn precursor. The NaCl was remove by washing with water and ethanol several times and

the final product (denoted as Sn/NMC) was obtained by drying in a vacuum at 60 °C overnight. The samples Sn/NMC-H and Sn/NMC-L were similarly synthesized, except that 4.5 g and 2.5 g SnCl₄·5H₂O were added, respectively. N-doped carbon microcages (denoted as NMC) were prepared without addition of SnCl₄·5H₂O. For comparison, sucrose was also used as carbon source instead of EDTA to obtain Sn/C (Sn in undoped carbon) composite.

Materials characterization: The structure of the samples were characterized by X-ray diffractometer (XRD, Bruker, D8 Diffractometer, Cu K α radiation = 0.154 nm) and Raman spectrometer (Raman, Renishaw, Reflex Raman instrument, laser excitation at 532nm). The morphology features were observed by scanning electron microscopy (FESEM, Hitachi, S-4800) and transmission electron microscopy (TEM, FEI Ltd, Tecnai F20). The X-ray photoelectron spectroscopy (XPS) spectra were evaluated by an imaging photoelectron spectrometer (Axis Ultra DLD, USA). Thermogravimetric analysis (TGA) was performed on a Perkin-Elmer Diamond analyzer with a heating rate of 10 °C min⁻¹ under air. The Brunauer–Emmett–Teller (BET) surface area and pore size distribution were analyzed using N₂ absorption on an ASAP 2020M (Micromeritics Instrument Corp., USA).

Electrochemical measurements: The electrochemical properties were evaluated using CR2032-type coin cells assembled in an argon-filled glovebox with lithium metal or sodium metal foils served as both the counter and reference electrodes. The working electrodes were composed of active material, carbon black (Super P), and carboxymethylcellulose sodium (CMC) with a mass ratio of 8:1:1 and cast onto the copper current collector. The loading density of the electrode is about 0.8 mg cm⁻². 1 M solution of LiPF₆ in ethylene carbonate/dimethyl carbonate (EC/DMC, 1:1 in volume with 5% fluoroethylene carbonate (FEC) as additive) and 1 M NaClO₄ in propylene carbonate (PC, with 5% fluoroethylene carbonate (FEC) as additive) were used as the electrolyte for LIBs and SIBs, respectively. The Celgard 2300 membrane and glass fiber were used as the separator for LIBs and SIBs, respectively. Galvanostatic charge/discharge tests were performed on a multichannel battery-testing system

(BT2000, Arbin Instruments, USA). Cyclic voltammetry (CV) curves were recorded on a Solartron 1470E Electrochemical Interface electrochemical workstation (Solartron Analytical, UK). Electrochemical Impedance Spectroscopy (EIS) was performed with the frequency ranging from 1 MHz to 0.01 Hz and an AC signal of 10 mV in amplitude as the perturbation using a Solartron 1470E electrochemical interface electrochemical workstation (Solartron Analytical, UK).

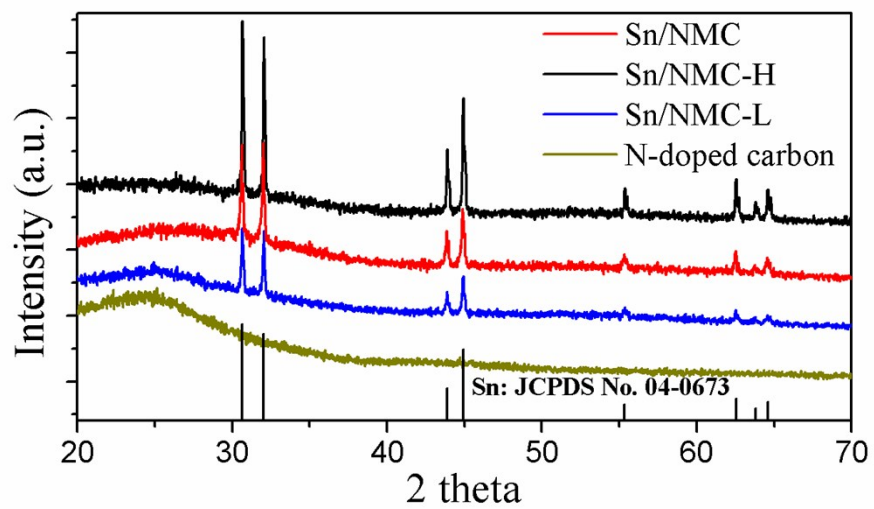


Fig. S1 XRD patterns of N-doped carbon microcages, Sn/NMC, Sn/NMC-H, and Sn/NMC-L composites.

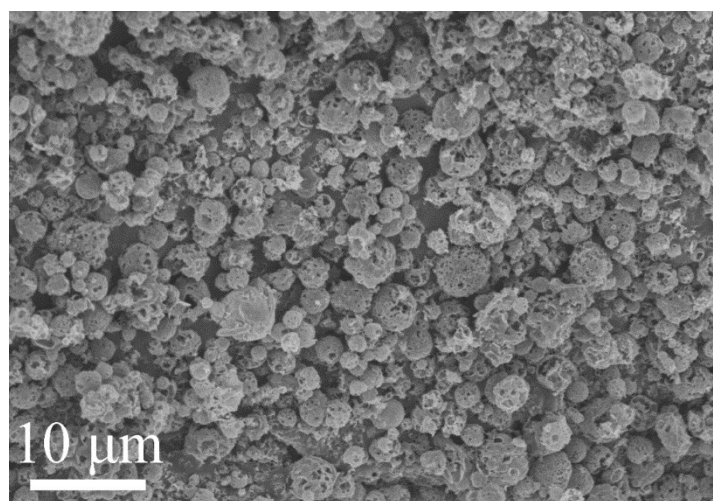


Fig. S2 SEM image of Sn/N-doped carbon microcages composite (Sn/NMC).

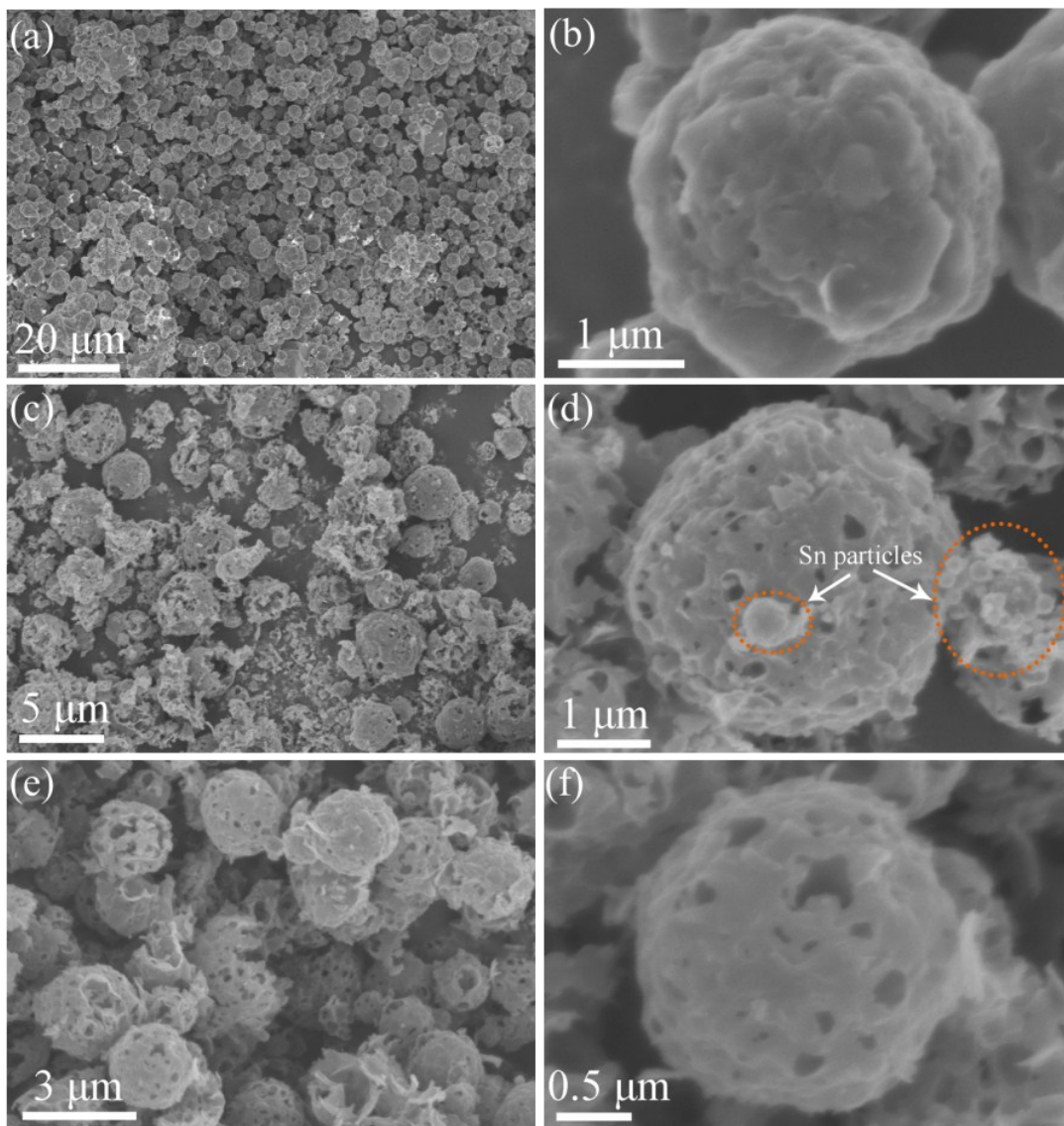


Fig. S3 SEM images of (a, b) Sn/NMC/NaCl before washing; (c, d) Sn/NMC-H composite; (e, f) Sn/NMC-L composite.

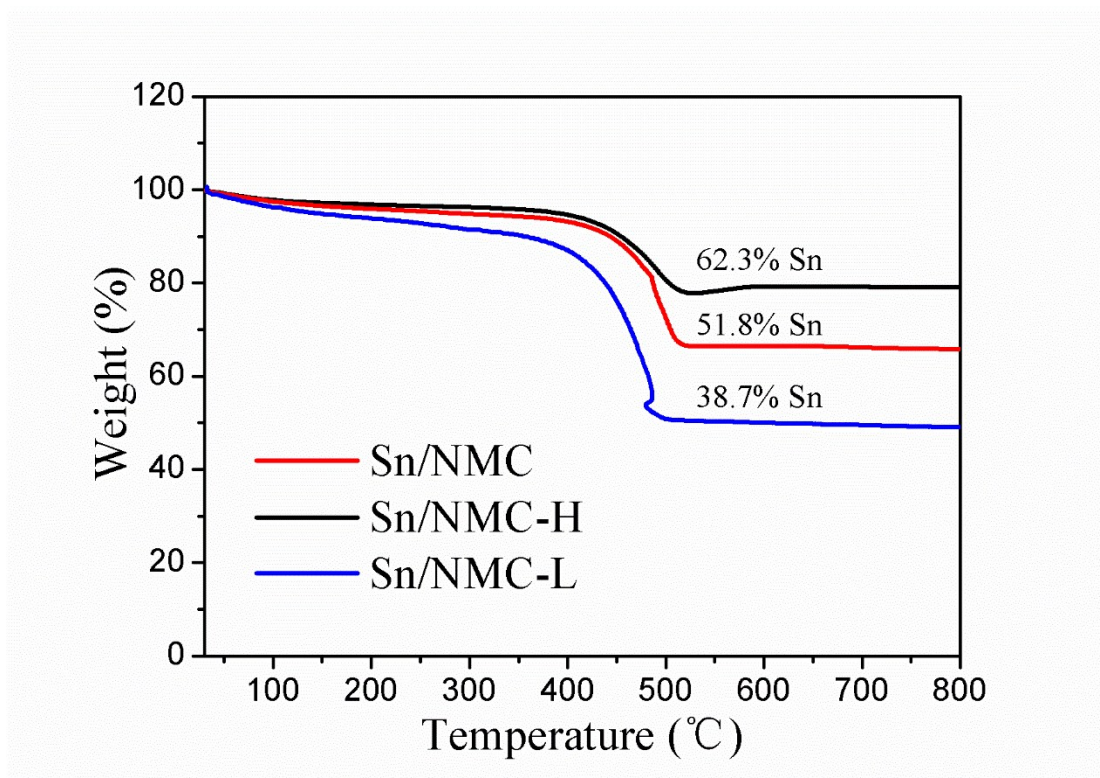


Fig. S4 TG curves of Sn/NMC, Sn/NMC-H, and Sn/NMC-L between 30-800 °C.

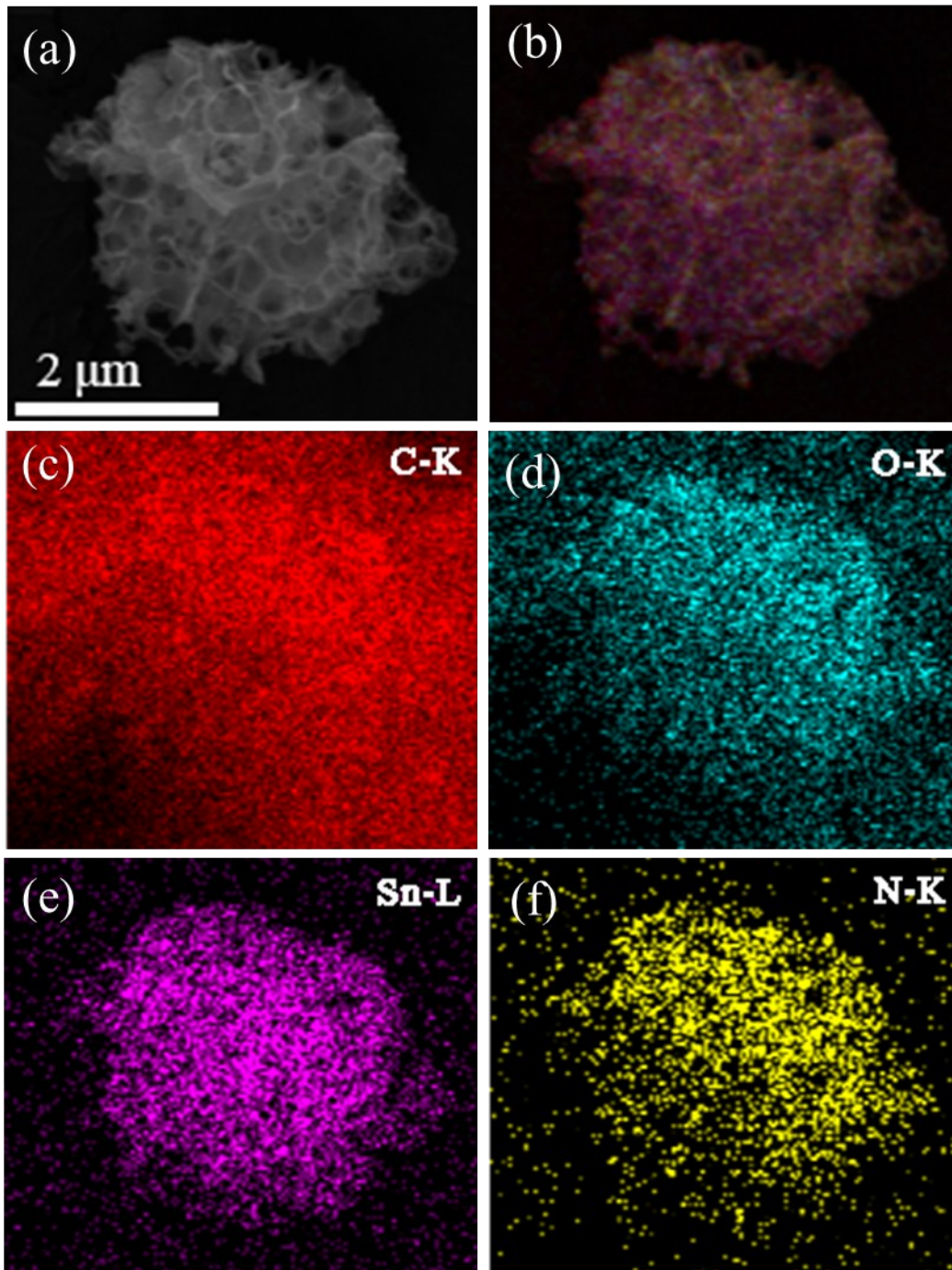


Fig. S5 (a) SEM image of Sn/NMC and (b) corresponding element mapping of (a); (c-f) element distribution of carbon, oxygen, tin, and nitrogen, respectively.

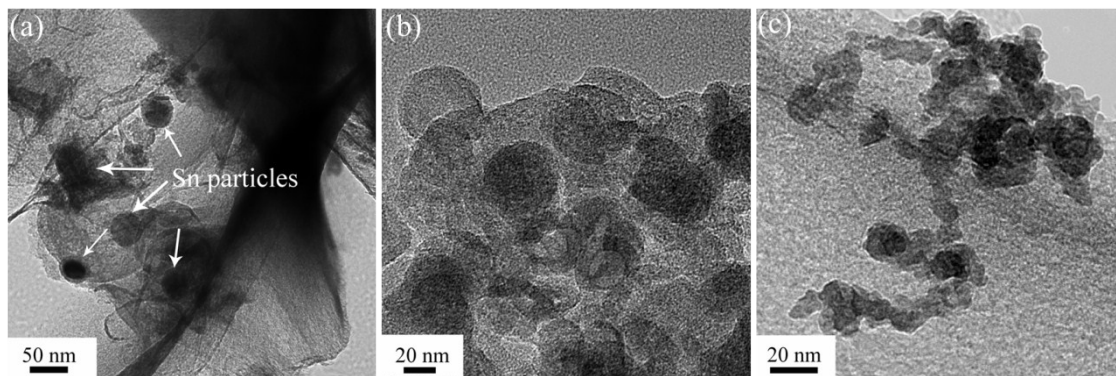


Fig. S6 TEM images of Sn/NMC-H with (a, b) sintering grown Sn particles dispersing on the surface of carbon; (c) Sn clusters adhering to the surface of carbon.

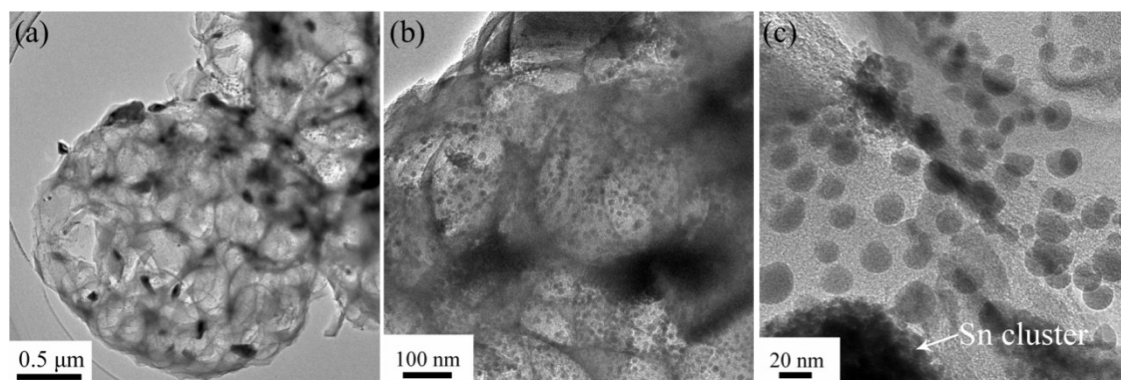


Fig. S7 (a-c) TEM images of Sn/C composite using sucrose as carbon source.

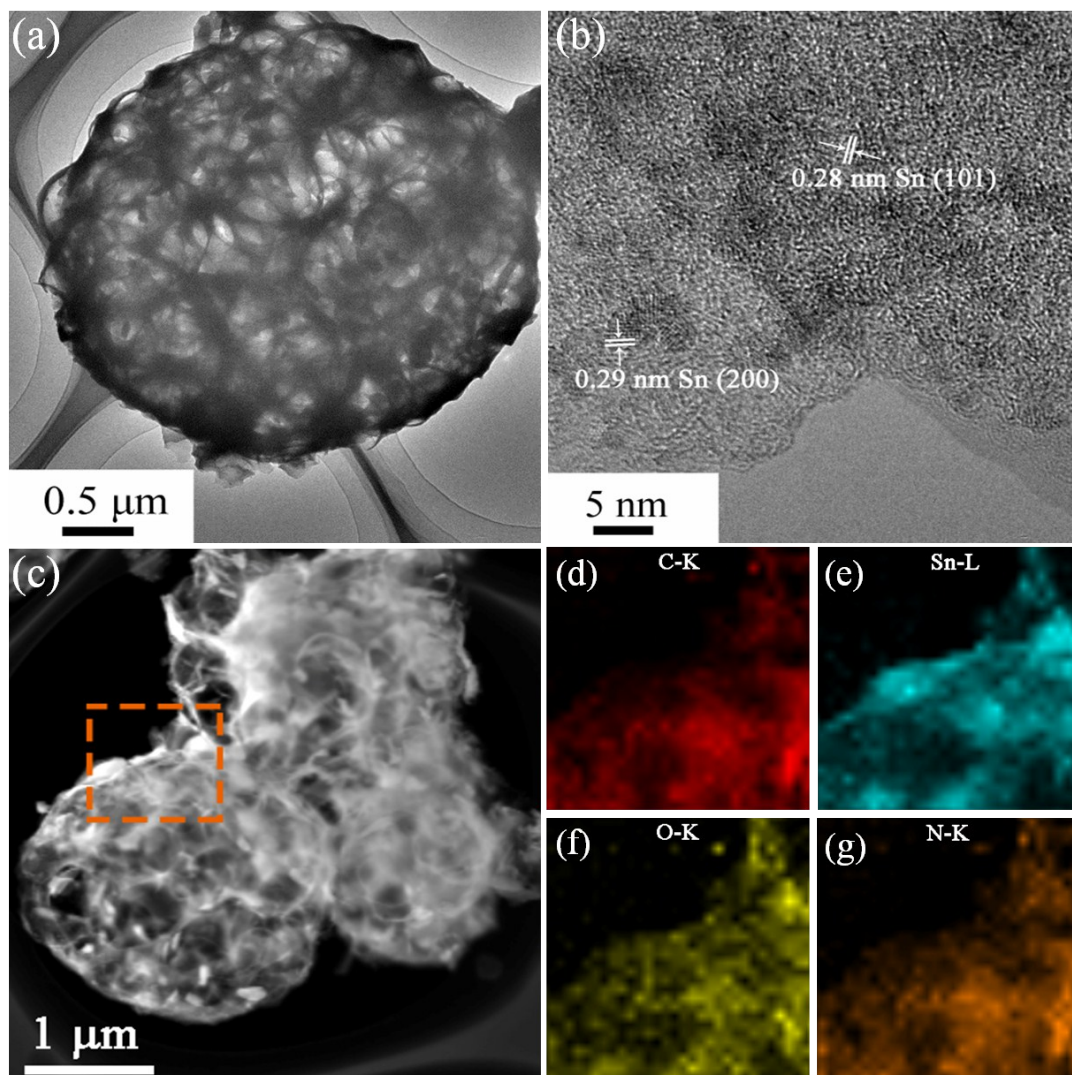


Fig. S8. (a) TEM and (b) HRTEM images of Sn/NMC; (c) HAADF-STEM image of Sn/NMC; (d-g) corresponding HAADF-STEM-EDS element mapping of the marked area in (c), for carbon, tin, oxygen, and nitrogen, respectively.

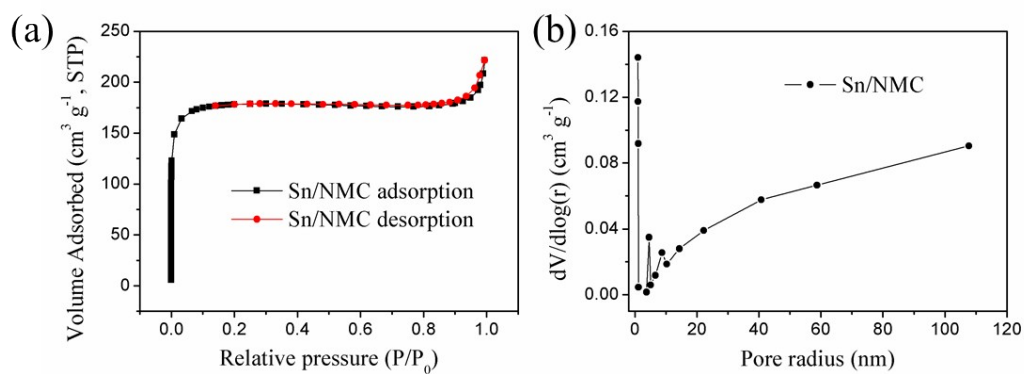


Fig. S9 (a) Nitrogen adsorption and desorption isotherms of Sn/NMC; (b) pore size distribution Sn/NMC.

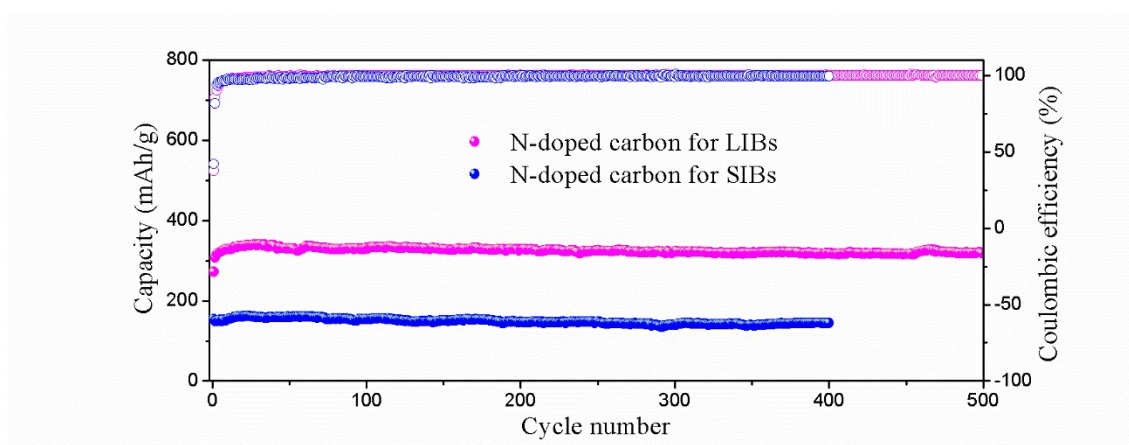


Fig. S10. Cycle performance of pure N-doped carbon microcages at 200 mA g^{-1} in LIBs and at 50 mA g^{-1} in SIBs.